Interaction of CO molecules with (Cu , Ag and Au) deposited on regular and defective MgO and BaO(001) surfaces: Density functional calculations

A. M. El Mahdy[a,*], H.O. Taha[a] , Kh.M. Eid[a], and S. Abdelhady[a]

[a]Department of Physics, Faculty of Education, Ain Shams University

*E-mail of the corresponding author: a_m_elmahdy@hotmail.com

Abstract

The adsorption properties and characteristics of CO on Cu, Ag and Au atoms deposited on various sites (regular O^{2-}, F_s^0 center, and F_s^+ center) of the alkaline earth oxide MgO and BaO. The three members of morphological irregularities, terrace, edge, and oxygen terminated corner of MgO and BaO (001) surface have been studied by means of density functional calculations and embedded cluster model. The examined clusters were embedded in the simulated Coulomb fields that closely approximate the Madelung fields of the host surfaces. The adsorption properties of CO have been analyzed with reference to the nature of the oxide support, pairwise and non-pairwise additivity, band gaps, associative adsorption, and electrostatic potentials. CO adsorption on an oxide support is drastically enhanced when CO is adsorbed on a metal deposited on this support. A dramatic change is found, and explained, when one compares the CO binding energy to O^{2-} and F_s^0 sites. The binding of CO precursor is mainly dominated by the $E_{(i)}^{TM-CO}$ pairwise additive contributions and the ε^{nadd} non-additivity term increases with increasing the basicity of the oxide support (MgO < BaO). While the classical contributions to the electrostatic interactions are quite similar for the deposited metals, they are quite dissimilar when going from defect-free to defect-containing surfaces.

Keywords: CO adsorption properties -Transition metals-Oxide supports- Density functional calculations

1.Introduction

Metal clusters and thin films on oxides play important roles in various technological applications, such as heterogeneous catalysis[1-7], gas sensors, corrosion-protective coatings, and microelectronic devices[8-14]. The adsorption, growth and electronic characteristics of metal ad-atoms deposited on oxides are of special interest because these factors are supposed to influence the physical and the chemical properties of metal clusters and to help optimize a catalytic process for the desired chemical reaction and product.

Oxide-supported metal clusters have been extensively studied from both the experimental and theoretical aspects[15-27]. Among the oxide supports, the MgO(001) surface, a prototype of the ionic-oxide surface, has been most widely investigated due to its favourable physical properties, such as its simple atomic structure, strong ionic bonding characteristics, and good chemical stability. The surface oxygen atoms of MgO(001) with a strong ionic character have valence states that are almost saturated. Recent high-level computational studies showed that on defect-free MgO (001) surfaces, metal ad-atoms preferred to adsorb on top of a surface oxygen atom[15-19]. For the experimental study of the properties of metal ad-atoms or clusters on oxides, ultra-thin oxide films supported by transition metals are more desirable and are widely used[23,28-29]. Pacchioni et al.[22], based on their density functional theory (DFT) calculations, showed that Au adsorbed more strongly on an Mo- supported MgO(001) surface than on an MgO (001) surface

The interaction of CO with MgO (001) surface, has received a great deal of attention in the literature[30-47]. It is considered a prototypical system for adsorption studies[44]. Moreover, since a number of metal oxides exist naturally in rocks and minerals exposed to groundwater and their presence influences the mobility of pollutants, the adsorption properties of this oxide have a geochemical relevance. Since CO is the most common probe molecule in surface science that has also been extensively used to characterize different MgO samples[48], we will examine the interaction of CO with electrons stabilized on the surface of MgO. We will consider F_s^0 sites, as well as a single electron trapped in an oxygen vacancy (positive charge F_s^+site).

The study of different transition metal atoms belonging to the same group (Cu Ag and Au) but have different valence structure can provide new information on the substrate–metal and metal–CO bonding, thus helping in the identification of surface defects where the metal atoms are stabilized. Cu, Ag and Au are representative of various transition metal atoms with complete d shell and partially filled s shell (Cu:$3d^{10}4s^1$, Ag:$4d^{10}5s^1$, Au:$5d^{10}6s^1$). Moreover, Cu, Ag, and Au are employed as active phases in a large group of catalytic systems.

Although in early works the support was supposed to be inert, nowadays it is well established that even for the less reactive supports changes in the properties of the adsorbate occur[49–65]. The presence and the quality of

the support for small clusters have been found to be of high relevance in the final catalytic activity. Some studies have assigned the variation of the adsorption properties to the increase of electron density due to the excess electron density on the oxygen atoms on more basic supports. The variation on the basicity of the support implies the modification of the chemical properties, and therefore deserves further investigation.

In this paper we present results on the adsorption properties and characteristics of CO on Cu, Ag and Au atoms deposited on various sites (regular O^{2-}, F_S^0 center, and F_S^+ center) of the alkaline earth oxide MgO and BaO. The three members of morphological irregularities, terrace, edge, and oxygen terminated corner of MgO and BaO (001) surface have been identified. These sites are illustrated in Fig. 1. Apart from the investigation of the role of defects present in the support in the deposited metal properties and CO binding energies, other basic questions related to the characteristics of adsorbate–substrate interactions have not been fully addressed yet. We have therefore paid special attention to bond order conservation theory, pairwise and non-pairwise additivity, associative adsorption, and electrostatic potentials.

2. Computational Details

Hybrid DFT and embedded cluster models have been used extensively to describe the electronic and geometrical structures of metal particles nucleated on regular and defective sites on metal oxide surfaces[66]. Sousa et al.[67] used a cluster/periodic comparison in the same computational model (DFT or Hartree–Fock) for the ionic systems MnO, FeO, CoO, NiO and CuO to establish that embedded cluster models provide an adequate representation. They used a lattice parameter (421 pm) for the bulk, with no surface relaxation or rumpling in the defect-free two-dimensional system, on the basis of a previous study.

A finite ionic crystal of 288 point charges was first constructed. The Coulomb potentials along the X and Y axes of this crystal are zero by symmetry as in the host crystal. The ± 2 charges on the outer shells were then modified by using a fitting procedure to make the Coulomb potential at the four central sites closely approximates the Madelung potential of the host crystal and to make the Coulomb potential at the eight points with coordinates $(0,\pm R,\pm R)$ and $(\pm R,0,\pm R)$ where R is half the lattice distance, which for MgO and BaO are 2.105, and 2.76Å respectively,, equal to zero as it should be in the host crystal. With these charges, 0.818566 and 1.601818, the Coulomb potential in the region occupied by the central ions is very close to that in the unit cell of the host crystal. The Coulomb potential was calculated to be (1.748) at the four central sites (compared with 1.746 for a simple cubic ionic crystal) and (0.0) at the previously defined eight points (compared with 0.0 for the same crystal). The low coordination (001) surface sites of the MgO and BaO crystals represented in Fig. 1 were then generated as follows:

(a) all charged centers with Cartesian coordinates ($\pm X$), ($\pm Y$) and (Z>0) were eliminated to generate a flat surface with 176 charged centers occupying the three- dimensional space ($\pm X$), ($\pm Y$), and (Z $\leq$ 0).

(b) all charged centers with Cartesian coordinates ($\pm X$), (Y< -1) and (Z> 0) were eliminated to generate an edge surface with 121 charged centers occupying the three-dimensional space ($\pm X$), (Y $\geq$ 1) and (Z $\leq$ 0);

(c) all charged centers with Cartesian coordinates (X> 1), (Y< -1) and (Z> 0) were eliminated to generate an O corner surface with 81 charged centers occupying the three-dimensional space (X $\leq$ 1), (Y $\geq$ -1) and (Z $\leq$ 0).

The clusters of Fig. 1 were then embedded within the central region of the crystal surface. All the electrons of the embedded clusters were included in the Hamiltonians of the *ab initio* calculations. Other crystal sites entered the Hamiltonians either as full or partial ionic charges as demonstrated previously[52].

Mg_nO_n and Ba_nO_n clusters have been used to model oxygen vacancies on several morphologic sites of the MgO and BaO (001) surface (Fig. 1): $Mg_{13}O_{13}$ and $Ba_{13}O_{13}$ for the terrace, consisting of two layers (first layer: Mg_4O_9; second layer: Mg_9O_4). Mg_9O_9 and Ba_9O_9 for the edge, Mg_6O_6 and Ba_6O_6 for the corner.

A neutral O vacancy was represented by $Mg_{13}O_{12}$ and $Ba_{13}O_{12}$ cluster for the terrace, leading to a cavity with two trapped electrons, i.e. a neutral diamagnetic F_S^0 center with the vacancy localized in the centre of the first layer. In this case, the geometrical optimization included the four central Mg and Ba atoms of first layer. Mg_9O_8 and Ba_9O_8 for the edge, Mg_6O_5 and Ba_6O_5 for the corner. A paramagnetic F_S^+ center was obtained from a neutral F_S^0 center by removing one electron from the periodic cell (Fig.1). Localization of the unpaired electron mainly in the vacancy region is corroborated by both quantum chemical calculations[68] and ESR experiments[69].

As far as the density functional model is concerned, density functional theory method was employed for the calculations of the adsorbate–substrate interactions[70]. The density functional theory calculations were performed by using Becke's three parameter exchange functional B3 with LYP correlation functional[71-72]. This B3LYP hybrid functional is based on the exact form of the Vosko–Wilk–Nusair correlation potential that is used to extract the local part of the LYP correlation potential[71-72]. Originally the functional B included the Slater

exchange along with corrections involving the gradient of the density[73] and the correlation functional LYP is that of Lee, Yang and Parr, which includes both local and non-local terms[74-75].

The Stevens, Basch and Krauss compact effective potential CEP basis sets[76-78] were employed in the present calculations. In these CEP basis sets, the double zeta calculations are referred to as CEP-31G, and similarly triple zeta calculations to as CEP-121G. Only one CEP basis set is defined beyond the second row, and the two sets are equivalent for these atoms. These basis sets have been used to calculate the equilibrium structure and spectroscopic properties of several molecules, and the results compared favourably with corresponding all-electron calculations. The computations reported in this paper were carried out by using Gaussian 03 system[79] and the molecular orbital densities were visualized by using the corresponding Gauss View software.

3. Results and discussion

3.1. Adsorption of single transition metal (TM) atom on O^{2-} sites

The first step in this study was to investigate the adsorption properties of a single transition metal atom; Cu, Ag and Au at the terrace, edge, and oxygen terminated corner of MgO and BaO (001) surface. The ad-atoms are deposited on the regular O^{2-} site. The surface cluster models have been chosen in such a way that the stoichiometry of MgO is retained. Thus, $Mg_{13}O_{13}$ and $Ba_{13}O_{13}$ cluster for the terrace, Mg_9O_9 and Ba_9O_9 for the edge, Mg_6O_6 and Ba_6O_6 for the corner are selected to simulate the basic sites where a metal atom will interact directly above an O^{2-} anion. These clusters contain two layers of ions and are further embedded in a suitable environment. For the $Mg_{13}O_{13}$ cluster (terrace) (Fig.1) contains four cations and nine anions in the first layer and four anions and nine cations in the second one. Similarly, the first layer of the Mg_9O_9 cluster (edge) (Fig.1) contains three cations and sex anions, whereas the second layer contains sex cations and three anions. The first layer of the Mg_6O_6 cluster (corner) contains two cations and four anions, whereas the second layer contains four cations and two anions.

We carried out calculations of adsorption energies E_{ads} per adatom at various adsorption sites. The adsorption energy was calculated as a difference of total energies. Here, E_{ads} was defined as

$$E_{ads} = E_{TM}MgO(001) - E_{MgO(001)} - E_{TM} \qquad (1)$$

Where $E_{TM}MgO(001)$ and $E_{MgO(001)}$ are the total energies of the TM- adsorbed and the clean MgO(001) surfaces, respectively and E_{TM} is the total energy of a free TM atom. Under this convention, a more negative value of the adsorption energy represents stronger adsorption.

The basic centre has been found to be the most reactive one versus metal adsorption in all the available studies for the MgO surface and therefore is likely to be the most reactive site for the whole series of alkaline earth oxides. In a systematic density functional study[38], the adsorption of single atoms of nine transition elements (Cu, Ag, Ni, Pd, Au, Cr, Mo, Pt, W) on the O^{2-} sites has been considered. In another study[16] the adsorption of single atoms of four transition elements (Cu, Ag, Ni, Pd) on the O^{2-} sites has been considered. In a more recent study, the adsorption of single atoms of seventeen transition elements (Cu, Ag, Au; Ni, Pd, Pt; Co, Rh, Ir; Fe, Ru, Os; Mn, Re; Mo, W) on the O^{2-} sites has been considered by Neyman et al.[56].

Table1 represents the equilibrium energetic and geometric parameters for the adsorption of single metal atom on MgO and BaO surfaces. The results reported in this table demonstrate that the adsorption energies for MgO surface on O^{2-} site follows the trend five coordinated surface < three-coordinated corner <four-coordinated step (edge) and for BaO surface on O^{2-} site follows the trend three-coordinated corner >four-coordinated step (edge) > five coordinated surface.

For the noble metal adatoms of Cu, Ag, and Au, the adsorption energies of -0.541,-0.394 and -0.557 eV for MgO surfaces, and -1.619, -1.048 and -2.057 eV for BaO surfaces were obtained, respectively. As shown in Table1, the equilibrium heights and adsorption energies of Cu, Ag, on O^{2-} of MgO surface are comparable with those reported by Jinwoo Park et al.[20] The quantitative changes observed are basically attributed to the different exchange correlation potentials and basis sets employed in the calculations. The adsorption energies of the Cu, Ag, and Au on O^{2-} sites increase with increasing the basicity of the oxide support from MgO to BaO. It is clear from Table1 that the adsorption energy at O^{2-} site of MgO and BaO (001) surface, increases according to the order Au > Cu > Ag.

The valence band of the MgO and BaO (001) surface with a highly ionic nature is well known to mainly consist of O 2p valence states that are almost saturated. The TM adatoms interact with the oxide surface atoms through the mixed bonding of the TM valence states with the 2p valence states of the surface O anion. The interatomic distances between the TM adatoms and the surface atoms of MgO and BaO (001), to which the TM adatoms were bound, well reflect the differences in interaction strength. For instance, a TM-O distance increases according to the order Ag < Au < Cu (see Table 1).

3.2. Adsorption of single transition metal (TM) atom on F_s^D sites

In the F_s^D vacancy, the two electrons of the (formal) dianion O^{2-} of the MO crystal are left at the surface and are localized in the cavity that was previously occupied by the now missing oxygen atom. A neutral F_s^D center with its vanishing electron affinity is expected to exhibit adsorption properties that, to a certain extent, resemble those of the regular O^{2-} sites of MO. Indeed, the interaction of TM adatoms on the F_s^D site is characterized by stronger binding energy with shorter equilibrium adsorption distance than on the surface O^{2-} site (Table1). The results reported in this table demonstrate that the adsorption energies for MgO and BaO (001) surface on F_s^+ site follows the trend three-coordinated corner > four-coordinated step (edge) > five coordinated surface. The adsorption energies are between -1.05 and -4.08 eV, and the strength of adsorption follows the order Au > Cu > Ag for each metal oxide support, and the order MgO < BaO for the considered surfaces. In the case of the O^{2-} site, the adsorbed atoms interact with the closed shells of an anion that is firmly kept in its position by ionic bonds with its neighbouring cations. That is quite different from adsorption on a defect F_s^D site, which is more like a hole with a low electron density inside that is easily polarizable. The electron density in the vacancy does not belong to any nucleus; the corresponding electronic states are stabilized via interaction with the vacancy environment, first of all with the nearest surrounding M cations. The stronger Pauli repulsions from the rigid MgO (001) walls are the reason why TM-O^{2-} bonds are weaker than TM-F_s^D bonds. These Pauli repulsions decrease when we go from MgO to BaO due to increasing the volume of the F_s^D cavity. Consequently, as shown in Table1 the binding energies of the three considered metals increase from MgO to BaO.

3.3. Adsorption of single transition metal (TM) atom on F_s^+ sites

The F_s^+ site of MO (001), compared with the F_s^D site, exhibit a differences: removal of an electron leaves on unpaired electron in the vacancy which is readily available for covalent bonding with an unpaired electron of a metal atom adsorbate, this factor is of particular importance for the M/F_s^+ complexes of Cu Ag and Au. These feature the most favourable electron configuration $(a_1)^2(a^*_1)^0$ and binding energies which are larger than those of their TM/F_s^D analogs with the configuration $(a_1)^2(a^*_1)^1$. All adsorption parameters of the present series of different metal atoms on F_s^+ centers, Table 1, are more uniform than those obtained on F_s^D centers. The results reported in this table demonstrate that the adsorption energies for MgO and BaO (001) surface on F_s^+ site follows the trend four-coordinated step (edge) > five coordinated surface > three-coordinated corner. The results are less adsorbate dependent, with an adsorption energy that goes from 2.39 to 3.31 eV and 2.71 to 4.22 eV respectively for MgO and BaO terrace surfaces. Compared with adsorption on F_s^D defect, the strength of the TM-F_s^+ bond is increased for the coinage metal atoms Cu, Au and Ag; coupling of their single valence s electron with the electron located in the cavity results in a rather strong covalent bond. In all cases, the positive charge associated to the defect leads to an additional contribution to the bonding from the metal polarization.

3.4. Adsorption of CO

First we have considered the adsorption properties of a CO molecule adsorbed with the C-end to the metal atom and the molecular axis normal to the surface plane, Fig.2. The energy characteristics of the gas-phase CO and M–CO are presented in Table 2. From this table one can see that the adsorption strength follows the order Au > Cu > Ag. The interatomic distances between TM and C atom of CO molecule are shorter for both Cu CO and Au CO complexes than those for Ag CO complexes.

The next step of adsorptivity calculations, is studying the adsorption of CO molecule via its C end on the defect free and defect-containing surfaces of MgO and BaO. The adsorption energies were calculated from the relations:

$$De(CO) = E(CO/X/MO) - E(CO) - E(X/MO) \qquad (2)$$

Where $De(CO)$ is the adsorption energy of CO on top of metal (X) deposited on a particular site on the surface of the metal oxide support, $E(CO/X/MO)$, site is the total optimized energy of the CO/X/MO substrate surfaces for either defect free or defect containing, $E(CO)$ is the optimal energy of CO and $E(X/MO)$ is the optimal energy metal (X) of deposited on a particular site of the oxide support. The results are represented in Table 3. The results reported in this table demonstrate that the adsorption energies for MgO and BaO (001) surface follows the trend four-coordinated step (edge) > five coordinated surface > three-coordinated corner. Several facts emerge from this table. First, the adsorption strength of CO/ BaO complexes is stronger than that of CO/MgO at the three adsorption sites; O^{2-}, F_s^D and F_s^+. This can be attributed to values of the band gaps of BaO and MgO terraces as that calculated in Table 7b. Moreover, the adsorption energies follow the order F_s^D < F_s^+ < O^{2-} for CO/MgO complexes and the order O^{2-} < F_s^D < F_s^+ for the CO/ BaO complexes. A second fact in Table 3, is that on contrary to the unbounded CO/O^{2-} site of MgO, the CO molecule is

highly bounded to the same site in BaO surfaces. As concluded in a comparative study by Giordano et al.[80] compared to the free MCO complexes, the deposition of MCO on the oxide sites resulted in enhancing back donation of charge. Such effect is more pronounced on F_S^0 centers where the electrons trapped in the cavity are more easily redistributed over the CO empty levels. On charged F_S^+ centers the presence of an electric field counteracts the effect of the back donation.

3.5. Adsorption of CO/TM/MO

The third step of adsorption properties was devoted to the adsorptivity of a single CO molecule via its C end on the transition metal atoms; Cu, Ag and Au deposited on the defect-free as well as defect-containing surfaces of MgO and BaO surfaces. The adsorption energies were calculated from the relations:

$$De(XCO) = E(CO/X/MO) - E(XCO) - E(MO) \qquad (3)$$

Where $De(XCO)$ is the adsorption energy of the XCO species on a particular site of the metal oxide support, $E(CO/X/MO)$, site is the total optimized energy of the CO/X/MO substrate surfaces for either defect free or defect containing, $E(XCO)$ is the minimal energy of the XCO species, and $E(MO)$ is the energy of the oxide support. The calculations have been performed within the C_{4v} symmetry constraint Table 4. The results reported in this table demonstrate that the adsorption energies for MgO and BaO (001) surface follows the trend three-coordinated corner > four-coordinated step (edge) > five coordinated surface. Some general trends can be deduced from the analysis of the results of Table 4. Ag does not exhibit tendency to bind CO. It should be mentioned that the gas-phase Ag–CO complexes are unbound, Table 2. For Ag/MgO this is consistent with the experimental observation that all CO has desorbed from the surface for temperatures around 120 K and that IR spectra are very similar for CO/MgO and CO/Ag$_1$/MgO[81-82]. The theoretical calculations of Giordano et al.[80] also report that Ag$_1$/MgO does not exhibit any tendency to bind CO. However, the situation is different for Cu and Au adsorbed on the oxide anions of the surfaces, Table 4. On Cu and Au, CO is strongly bound to the metal atoms adsorbed on oxide anions. In these cases the CO adsorption energies are increases in the order Au (0.87eV) < Cu (–0.83eV) and in the order Au (-0.50 eV) < Cu (–1.09eV) at the O^{2-}site of MgO and BaO, respectively. The strength of adsorption follows the order Cu > Au for each metal oxide support, and the order MgO < BaO for the considered series. In other words, the strength of adsorption increases with increasing the basicity of the oxide support. Thus, CO is expected to desorbed from oxide anions well above room temperature. The metal–CO bond strength, is considerably enhanced when the metal is supported to the oxide surface, Tables 2 and 4. It also increases with increasing the basicity of the oxide support.

Now we have considered the adsorption of CO on the metal atoms deposited on F_S^0 centers. The F_S^0 center is an anion vacancy occupying two electrons. Here, again, the calculations have been performed within the C_{4v} symmetry constraint, and some general trends can be deduced from the analysis of the results of Table 4. Ag exhibits tendency to bind CO. Again the adsorption energies for MgO and BaO (001) surface follows the trend three-coordinated corner >four-coordinated step (edge) > five coordinated surface. The adsorption energies are between - 0.19 and -1.20 eV, and the strength of adsorption follows the order Cu > Au >Ag for each metal oxide support and the order MgO < BaO for the considered series.

The second group of defect sites considered in this study is that of the paramagnetic F_S^+ centers. These consist of a single electron trapped in the anion vacancy; their electronic structure has been studied in detail in polycrystalline MgO samples by ESR spectroscopy [83-84]. On these sites, Ag does not exhibit tendency to bind CO relative to other metals. Despite the fact that CO is strongly bound on Au, and Cu deposited on F_S^+, no clear trends are shown regarding the strength of binding energies. The M–CO bonding is weaker than that of the complex with the defect. Not surprisingly, the major differences in electronic structure caused by the positive charge of the vacancy are reflected on the binding properties of CO and MCO.

3.6.Pairwise and non-pairwise additivity

In studying a supported-metal catalyst system, it is very important to quantify the extent to which the support (S: MgO or BaO) affects the interaction of the CO ad-molecule with the transition metal atom. The interaction energy $E_{(i)}^{S-TM-CO}$ among three subsystems; the support (S), transition metal (TM), and the adsorbate (CO) molecule can be defined as:

$$E_{(i)}^{S-TM-CO} = E^{S-TM-CO} - E^S - E^{TM} - E^{CO} \qquad (4)$$

where every energy on the right-hand side of Eq.(2) is calculated using geometrical parameters corresponding to the equilibrium geometry of S.M.CO.E(i) $^{S.M.CO}$ is the energy required to separate three subsystems without changing their geometrical parameters. This energy can be decomposed into three pairwise components and a non-additive term E^{nadd}

$$E^{S-TM-CO}_{(i)} = E^{S-TM}_{(i)} + E^{S-CO}_{(i)} + E^{TM-CO}_{(i)} + \varepsilon^{nadd} \qquad (5)$$

The non-additivity ε^{nadd} term[85-86] is a measure of cooperative interactions among the subsystems. The four energy terms on the right-hand side of Eq. (5) are calculated from the relations:

$$E^{S-TM}_{(i)} = E^{S-TM} - E^{S} - E^{TM} \qquad (6)$$

$$E^{S-CO}_{(i)} = E^{S-CO} - E^{S} - E^{CO} \qquad (7)$$

$$E^{TM-CO}_{(i)} = E^{TM-CO} - E^{TM} - E^{CO} \qquad (8)$$

$$\varepsilon^{nadd} = E^{S-TM-CO}_{(i)} - E^{S-TM}_{(i)} + E^{S-CO}_{(i)} + E^{TM-CO}_{(i)} \qquad (9)$$

In Table 5 we present total interaction energies for the S.M.CO system, pairwise energy components, and the non-additive energy terms as defined in Eqs. (4) – (9). Many facts can be explored from this table: (i) the small values of magnitude of $E^{S-CO}_{(i)}$ pairwise component, representing the interaction energy between support (S) and admolecule (CO) in the S-TM-CO system may be attributed to the large separation between (S) and the CO ad-molecule. This result means that the binding of CO is mainly dominated by the $E^{TM-CO}_{(i)}$ term. However, it should be mentioned that the smaller $E^{TM-CO}_{(i)}$ values does not mean that the CO is weakly bounded to the support (S), as a result of the large separation between CO and the support (S) considered in calculating this component, this is simply because such distance does not represent the real equilibrium interatomic distance that corresponds to the global minimum on the potential energy surface. (ii) The second fact in Table 5 is that the ε^{nadd} term which is a measure of cooperative interactions among the subsystems, increases with surface defect-formation (with all TMs) and with increases the electrical conducting properties of support (MgO < BaO). Consequently, we can conclude that the interaction of CO with TM atom is essentially influenced by these two factors; defect formation and the electrical conductivity of the support. The data in Tables 2 and 5 provide further support for this observation by showing that the value of d(TM–C) in the TM-CO and S-M-CO systems differs significantly. Furthermore, the binding of CO on the TM and for the S-TM-CO system differs significantly too. Consequently, we can conclude that the interaction of CO with TM atom is essentially influenced by these two factors; defect formation and the electrical conductivity of the support.

We have considered the possible associative or dissociative adsorption reactions of CO at the defect-free and defect-containing surface sites of the title oxides:

$$OC + X - S \rightarrow O + C..X - S \qquad (10)$$
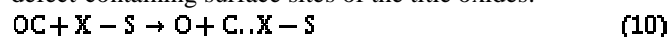
where X represents the adsorption site: O^{2-}, F^{0}_{S} or F^{+}_{S}. The released energy ΔE was calculated from the relation

$$\Delta E = \sum E_{products} - \sum E_{reactants} \qquad (11)$$

The reactions energetic are compiled in Table 6, and it can be obviously seen that these reactions, for CO at different sites and supports, are all calculated to be endothermic. Namely, the assumed associative adsorption reactions are energetically favourable. However, the tendency toward the dissociative behaviour increases with defect formation and with increasing the basicity of the oxide support, i.e., the released energy gets less positive. This tendency is concomitant with increasing the strength of the C.X bond in C.X–S structure, Table 3.

The data in Tables 7a–7c represent band gap calculations as the differences between the tops of valence band and bottoms of conduction bands of the defect-free surfaces and as the differences between the HOMOs and LUMOs of the defect-containing surfaces for the TMCO complexes (Table 7a); TM/MO (Table 7b), and CO/TM/MO (Tables 7c). The data in Table 7b for the free substrate of MgO (0 0 1) surface show that the values of band gaps decrease according to the order; F^{+}_{S} (−3.78 eV) > O^{2-} (−3.34 eV) > F^{0}_{S} (−1.94 eV).

However, upon the adsorption of TM/MgO, it can be seen from the data in Table 7b that there is a reduction in the values of band gaps for all metals at the O^{2-}, F^{0}_{S} and F^{+}_{S} sites. The band gaps decrease in the order Au (−2.38 eV) > Cu (−1.93 eV) > Ag (−1.83 eV) at the O^{2-} and in the order Au (−0.98 eV) > Cu (−0.71 eV) > Ag (−0.68 eV) at the F^{0}_{S} site and in the order Cu (−3.65 eV) > Ag (−3.59 eV) > Au (−3.37 eV) at the F^{+}_{S} site.

Moreover, upon the adsorption of CO/TM/MgO (0 0 1), with the exception of a slight increase in the case CO/TM/MgO (TM = Cu, Ag and Au), a sharp decrease in the band gaps are observed for all TM/O^{2-} and F^{0}_{S} sites. Such decrease follows the order Au (−1.22 eV) > Ag (−1.20 eV > Cu (−0.41 eV) , while at the F^{0}_{S} site the order is Cu (−0.92 eV) > Au (−0.82 eV) > Ag (−0.78 eV) . Contrary to the O^{2-} and F^{0}_{S} sites, an increase in the values of band gaps is recorded at the CO/TM/F^{+}_{S} sites compared to

those of the F_S^+ site of MgO (0 0 1) surface. Such increase follows the order Ag (–3.67 eV) > Au (–3.54 eV) > Cu (–3.38 eV) for the F_S^+ site, respectively.

Regarding the values of band gaps of TM/BaO (0 0 1), Table 7b, that is; a reduction in the band gaps at both F_S^0 and F_S^+ sites of TM/BaO with respect to those of BaO surface. While an increase in the band gaps is observed for at the O^{2-} site of TM/BaO. For the F_S^0 and the F_S^+ sites the decrease in band gaps follows the and Ag (–0.43 eV) > Cu (–0.42 eV) > Au (–0.41 eV), the order Au (–1.70 eV) > Ag (–1.69 eV) > Cu (–1.68 eV). respectively, while at the O^{2-} site, the decrease in the band gaps follows order Au (–0.96 eV) > Ag (–0.94 eV) > Cu (–0.87 eV)

However, upon the adsorption of CO/TM/BaO (0 0 1), the data in Tables 7c show that, at the O^{2-} and F_S^0 sites there is a reduction in the band gaps for all TMs. At the F_S^+ site there is an increase in the band gaps upon the adsorption of CO/TM/ BaO (0 0 1) for all metals. One can see that there is nearly a consistency between the band gap results and the adsorption energies.

Fig.3, plots the HOMOs, of the MO (MgO: Fig.3a; and BaO:Fig.3b), TM/MO, and CO/TM/MO. One can recognize the polarization induced by adsorption, and the distortion occurred in the F_S^0 and F_S^+ centers (s-like shape). The figure confirmed the results in Tables7a–7c and the adsorption properties discussed above. It is clear from Fig.3a that, there is a difference in the shape of HOMO of the three adsorption sites; O^{2-}, F_S^0, and F_S^+. The HOMO for the oxygen vacancies F_S^0 and F_S^+ has a large s-like character. The increase in adsorption height observed in Ag/MgO (2.73 Å) can contribute to the Pauli repulsion of the metal valence electrons with those in the p-orbital's of the surface oxygen atom. Therefore, the HOMO of Ag/O^{2-} complex has the characteristics of an antibonding orbital. However, upon the adsorption of Ag/F_S^0 and Ag/F_S^+ sites, the interatomic distances are reduced leading to a larger overlaps between the HOMO of MgO and LUMO of Ag atom. Moreover, upon the adsorption of CO/Ag/MgO, the Ag - S distance decreases at the O^{2-} as well as F_S^0 sites and increases at the F_S^+ site. Consequently, one can recognize the stronger polarization in both cases; O^{2-} and F_S^0 site than that at the F_S^+ site of the HOMO of MgO and LUMO of Ag of the complex CO/Ag/MgO.

A similar behaviour is observed for the BaO systems (BaO, Ag/BaO, and CO/Ag/BaO) keeping in mind the smaller band gaps of the BaO surfaces.

It is necessary to analysis the bonding mechanism and confirming the above results in qualitative and quantitative aspects. For this reason, the total charge-density contours in the (0 0 1) plane of the free substrate MO (MgO and BaO), Ag/MO (as a representative for the other TM), and CO/Ag/MO systems are shown in Fig.4. These contours clearly show that the changes in the charge density are restricted to both the adsorbates; CO molecules as well as Ag, and the adsorption sites (O^{2-}, F_S^0, and F_S^+), while the rest of oxide remains unperturbed. In other words, the charge distribution in the sub interface layer and in the lower half of the interface layer is nearly identical to that in the bulk-like center layer. A result means that the bonding has a very local nature. It should however, mentioned that, the same behavior was observed for the other transition metal atoms (Cu, Au).

It is generally accepted that the electrostatic potential plays a key role in the interactions of adsorbates with ionic substrates. In order to understand the possible electrostatic contributions to adsorbate–substrate interactions, the electrostatic potentials (ESP) over the oxygen anion (O^{2-}) site of the defect-free terrace surfaces and the anion vacant (F_S^0 and F_S^+) sites of the defect containing surfaces of variable sizes have been calculated and presented in Fig.5, for both oxides (MgO and BaO). From this figure, it is observed that the electrostatic potential depends significantly on the cluster size, where the strength of the electrostatic potentials follows the order terrace > edge > corner in consistence with the results of Ferrari and Pacchioni[87]. This indicates that the electrostatic potentials of the defect free and defect containing surfaces were very different and the shapes of the functions were very dissimilar. On the other hand, the trend of the electrostatic potentials follows the order O^{2-} > F_S^0 > F_S^+. Since the electrostatic interaction of an admolecule with the surface will mainly consist of electric field induced dipole and electric field derivatives-induced quadrupole moments, one expects that the classical contributions to the admolecule–surface interactions are quite different going from the defect free to the defect containing surfaces. Curve crossings that occur at about 1 Å imply that the electrostatic interactions are identical regardless of the nature of the surface, defect free or defect containing.

The alteration of bond strength of the support–MCO fragment on O^{2-}, F_S^0 and F_S^+ sites of the oxide support can be understood and rationalized with simple orbital schemes that include the highest occupied molecular orbitals (HOMOs) and the lowest unoccupied molecular orbital's (LUMOs) of the oxide support. In Table7 we list the HOMOs and LUMOs of MCO fragments together with the HOMOs and LUMOs of the defect-free and defect-containing surfaces of the oxide supports. These data were then further represented graphically in Fig. 6. As shown from Table7, and Fig. 6, the reactivity of the deposited MCO fragments on the various sites of oxide supports increases significantly (from MgO to BaO) with decreasing the value of the energy gap (HOMO–

LUMO) of the substrate. In other words there is a linear correlation between the strength of the support–MCO bond and the basicity of the crystal. For example, consider the adsorption energies of CuCO fragment on the O^{2-} site of MgO and BaO. The energy gaps HOMO –LUMO decreases from –3.34 eV for MgO, to – 0.88 eV for BaO. The corresponding adsorption energies (bond strengths) of CuCO fragment increases simultaneously from –1.29 eV on MgO, to –3.42 eV on BaO. This is applied equally well to the whole set of MCO fragments on the examined oxide supports. The results are in line with increasing the basicity of the oxide support, and with the amount of charge transferred from the O^{2-} anion of the oxide support to the MCO adsorbate.

4.Conclusion

In this study, the adsorption structures and electronic properties of the CO molecule on the TM atoms (Cu, Ag and Au) deposited on F_s^0 and F_s^+ defect sites as well as on regular O^{2-} of the alkaline earth oxide MgO and BaO (001) surfaces at low coordinated surface was studied by DFT and the embedded cluster approach. The three members of morphological irregularities, terrace, edge, and oxygen terminated corner of MgO and BaO (001) surfaces have been identified. The model clusters were embedded in simulated Coulomb fields that closely approximate the Madelung fields of the host surfaces, and the adsorption properties have been analyzed with reference to the bond order conservation energy, pairwise and non-pairwise additivity, associative adsorption, and electrostatic potentials. The adsorption of CO on a metal in the gas-phase or on an oxide support is drastically enhanced when CO is adsorbed on a metal deposited on this oxide support. While Ag does not exhibit tendency to bind CO on the defect-free surface, on Cu and Au CO is strongly bound. The strength of CO adsorption increases with increasing the basicity of the oxide support so that CO is expected to desorb from oxide anions well above room temperature. The metal–CO bond strength, is considerably enhanced when the metal is supported to the oxide surface. While Cu atoms are bound at the oxide anions of the defect-free surface, Au atoms are bound at the F_s^0 centers of the defect-containing surface. The interaction of CO with the metal M is essentially affected by two factors, defect formation and basicity of the support. The reactions, for CO at different sites and supports, are all calculated to be endothermic. The oxide support surface has a considerable effect on the interaction of CO with the metal and its role is not restricted to supporting the metal but also influences the interaction of the CO molecule with the TM atoms. The binding of CO is dominated by the $E(i)_{M.CO}$ term, and the non-additivity increases with increasing the basicity of the support. While the classical contributions to the adsorbate–surface interactions are quite similar for the deposited transition metals, they are quite different when going from defect-free to defect-containing surfaces. In the framework of the basicity of the support, the electrostatic potential generated by the oxide modifies the physical and chemical properties of the adsorbed metal and therefore its reactivity versus the CO adsorbate.

References

[1] Bond G C and P A Sermon (1973). Gold Catalysts for Olefin Hydrogenation. *Gold Bull*.6, 102.
[2] Haruta M, Yamada N, Kobayashi T and Iijima S (1989). J. Catal. 115,301.
[3] Haruta M, Tsubota S, Kobayashi T, Kageyama H, Genet J J, and Delmon B (1993).J.Catal.144,175.
[4]] Haruta M(1997).Catal. Today 36,153.
[5] Campbell C T(1997).Surf. Sci. Rep 27,1.
[6] Freund H J(1997). Angew. Chem.109,444.
[7] Valden M, Lai X, and Goodman D W(1998). Science281,1647.
[8] Urano T. and Kanaji T(1988). J. Phys. Soc. Jpn.57,3403.
[9] Butler W. H., Zhang X.-G., Schulthess T. C., and MacLaren J. M(2001).Phys. Rev. B63, 054416.
[10] Yuasa S, Nagahama T., Fukushima A., Suzuki Y., and Ando K(2004). Nat. Mater.3,868.
[11] Yuasa S(2008).J. Phys. Soc. Jpn.77,031001.
[12] Yu B D and Kim J S(2006).Phys. Rev. B73,125408.
[13]Yeo J N, Jee G M, Yu B D, and Choi B C(2008). J. Korean.Phys.Soc.52,1938.
[14] Yang L H, Park J, Yu B D, and Jang Y R(2010).J. Korean Phys. Soc.56 ,791.
[15] Musolino V, Selloni A, and Car R(1998).J. Chem. Phys.108,5044.
[16] Matveev A V, Neyman K M, Yudanov I V, and Rosch N(1999). Surf. Sci.426,123.
[17] Bogicevic A and Jennison D R (1999).Surf. Sci.437, L741.
[18] Sljivancanin Z and Pasquarello A(2003).Phys. Rev. Lett.90,247202.
[19] (2005).Phys. Rev. B71,193403.
[20] Park J and Yu B D(2008). J. Korean Phys. Soc.53,1976.
[21] Park J, Park I, and Yu B D(2009).J. Korean Phys. Soc.54,109.
[22] Pacchioni G, Giordano L, and Baistrocchi M(2005). Phys. Rev. Lett.94 ,226103.
[23] Kulawik M, Nilius N, and Freund H J(2006).Phys. Rev. Lett.96,036103.
[24] Sterrer M, Risse T, Pozzoni U, Giordano L, Heyde M, Rust H P, Pacchioni G, and Freund H J(2007). Phys. Rev. Lett.98,096107.

[25] Honkala K and Ha¨kkinen H(2007).J. Phys. Chem. C111, 4319.

[26] Park J , Yu B D and Kim H(2009).Phys. Rev. B79, 233407.

[27] Sicolo S, Giordano L, and Pacchioni G(2009).J. Phys. Chem. C113,16694.

[28] Jaeger R M, Kuhlenbeck H, Freund H J, Wuttig M, Hoffmann W, Franchy R,Ibach H(1991). Surf.Sci.259,235.

[29] Libuda J, Winkelmann F, Bäumer M, Freund H J, Bertrams Th,Neddermeyer H, Müller K (1994).Surf.Sci.318,61.

[30] Furuyama S, Fujii H, Kawamura M, Morimoto T(1978). J. Phys. Chem.82, 1028.

[31] Paukshtis E A, Soltanov R I, and Yurchenko N E(1981). Reaction Kinet.Catalysis Lett. 16, 93.

[32] Henry C R, Chapon C, and Duriez C(1991). J. Chem. Phys. 95,700.

[33] He J W, Estrada C A, Corneille J S, Ch Wu M, and Wayne Goodman D(1992). Surf. Sci.261,164.

[34] Colbourn E A and Mackrodt W C(1984). Surf. Sci. 143, 391.

[35] Pope S A, Hillier I H, Guest M F, Colbourn E A, and Kendrick J(1984). Surf. Sci. 139, 299.

[36] Pacchioni G. and Bagus P. S(1993). Adsorption on Ordered Surfaces of Ionic Solids and Thin Films, Eds. H.-J. Freund and E. Umbach, Vol. 33, Springer Series Surf.Sci., Springer-Verlag, Berlin.

[37] Neyman K. M, Ruzankin S Ph, and Rösch N(1995). Chem. Phys. Letters 246, 6, 546.

[38] Yudanov I V, Nasluzov V A, Neyman K M, Rösch N(1997). Int. J. Quant. Chem. 65, 975.

[39] Nygren M A and Petterson L G M(1996). J. Chem. Phys.105,9339.

[40] Wichtendahl, M. Rodriguez-Rodrigo, U. Härtel, H. Kuhlenbeck, and H.-J. Freund (1999).Phys.Stat. Sol. (a) 173,93.

[41] Snyder J A, Alfonso D R, Jaffe J E, Lin Z, Hess A C, and Gutowski M(2000). J. Phys. Chem. B, 104, 4717.

[42] Soave R, and Pacchioni G(2000).Chem. Phys. Letters, 320, 345.

[43] Sallabi K, and Jack D B(2000). J. Chem. Phys., 112, 5133.

[44] Dohnálek Z, Kimmel G, Joyce S A, Ayotte P, Smith R S and Kay B D(2001). J. Phys. Chem B 105, 3747.

[45] Rodriguez J A, Jirsak T, Perez M, Gonzalez L, Maiti A(2001). J. Chem. Phys. 114, 4186.

[46] Damin A, Dovesi R, Zecchina A, Ugliengo P(2001). Surf. Sci. 479, 255.

[47] Xu Y., Li J., Zhang Y., and Chen W(2003). Surf. Sci. 525,13.

[48] Spoto, G.; Gribov, E. N.; Ricchiardi, G.; Damin, A.; Scarano, D.; Bordiga, S.; Lamberti, C.; Zecchina, (1994)Progress in Surface Science., 76,71.

[49] Henrich V.E., Cox P.A(1994).The Surface Science of Metal Oxides, Cambridge University Press, Cambridge,.

[50] Pacchioni G(2002). Surf. Sci. 520, 3.

[51] Lambert R, Pacchioni G(1997).Chemisorption and Reactivity of Supported Metal Clusters and Thin Films, NATO ASI Series E, vol. 331, Kluwer,Dodrecht.

[52] Abdel Halim W S, Abdel Aal S, Shalabi AS(2008).Thin Solid Films 516, 4360.

[53] Wang Y, Florez E, Mondragon F, Truong TN(2006). Surf. Sci. 600 , 1703.

[54] Lopez N, Illas F(1998). J. Phys. Chem. B 102 ,1430.

[55] Gronbeck H, Broqvist P(2003)., J. Phys. Chem. B 107,12239.

[56] Neyman K.M., Inntam C., Matveev A.V., Nasluzov V.A., Rösch N(2005). J. Am. Chem. Soc. 127,11652.

[57] Chiesa M, Giamello E, Di Valentin C, Pacchioni G, Sojka Z,van Doorslaer S(2005). J. Am. Chem. Soc. 127 16935.

[58] Colbourn E.A(1999). C.R.A. Catlow (Ed.), Advances in Solid State Chemistry, vol. I, JAI Press, London.

[59] Me´ne´trey M, Markovits A, Minot C(2007). J. Mol. Struct. Theochem.808,71.

[60] Stoneham A.M (1975). Theory of Defects in Solids, Oxford University Press.

[61] Vail J M, Pandey R, Kunz A B(1992). Revs. Solid State Sci. 5, 24.

[62] Hakkinen H, Manninen M(1996). J. Chem. Phys. 105 10565.

[63] Nygren M.A, Petterson L G M, Barandiaran Z , Seijo L(1994). J. Chem. Phys. 100 ,2010.

[64] Mejias J A(1996).Phys. Rev. B 53,1028.

[65] Ferrari A M, Roetti C, Pisani C(2007). Phys. Chem. Chem. Phys. 9, 2350.

[66] Eid K M, Taha H O,Kamel M A , Ashour A E , Abdel Halim W S (2012). Appl. Surf. Sci. 258 , 9876.

[67] Sousa C, Graaf C, Lopez N, Harrison N M , Illas F(2004). J. Phys. Condens. Matter 16, S2557.

[68] Ferrari A M, Pacchioni G(1995). J. Phys. Chem.99,17010.

[69] Tench A J, Nelson R L(1968). J. Colloid and Interface Science 26 ,364.

[70] Kohn W, Sham L(1965).J. Phys. Rev. A 140, 1133.

[71] Becke A D(1993). J. Chem. Phys. 98 ,5648.

[72] Vosko S.H, Wilk L, Nusair M(1980). Can. J. Phys. 58,1200.

[73] Becke A D(1988). Phys. Rev. A 38 ,3098.

[74] Lee C, Yang W, Parr R G(1988). Phys. Rev. B 37, 785.

[75] Miehlich B, Savin A, Stoll H, Preuss H(1989).Chem. Phys. Lett. 157, 200.

[76] Stevens W, Basch H, Krauss J(1984).J. Chem. Phys. 81,6026.

[77] Stevens W, Krauss M, Basch H, Jasien P G(1992). Can. J. Chem. 70, 612.

[78] Cundari T R, Stevens W J(1993). J. Chem. Phys. 98,5555.

[79] Frisch, M.J., Trucks, G.W., Schlegel, H.B., Scuseria, G.E., Robb, M.A., Cheeseman, J.R., Zakrzewski, V.G., Montgomery, J.A., Stratmann, R.E., Burant, J.C., Dapprich, S., Millam, J.M., Daniels, A.D., Kudin, K.N., Strain, M.C., Farkas, O., Tomasi, J., Barone, V., Cossi, M., Cammi, R., Mennucci, B., Pomelli, C., Adamo, C., Clifford, S., Ochterski, J.,Petersson, G.A., Ayala, P.Y., Cui, Q., Morokuma, K., Malick, D.K., Rabuck, A.D., Raghavachari, K., Foresman,J.B., Cioslowski, J., Ortiz, J.V., Stefanov, B.B., Liu, G., Liashenko, A., Piskorz, P., Komaromi, I., Gomperts, R., Martin, R.L., Fox, D.J., Keith, T., Al-Lamham, M.A.,Peng, C.Y., Nanayakkara, A., Gonzalez, C., Challacombe, M., Gill,P.M.W., Johnson, B.G., Chen, W., Wong, M.W., Andres, J.L., Head-Gordon, M., Replogle, E.S. and Pople, J.A. (2004)Gaussian. Wallingford CT, Inc., Wallingford.

[80] Giordano L, Vitto A D, Pacchioni G , Ferrari AM(2003). Surf. Sci.540, 63.

[81] Wichtendahl R, Rodriguez-Rodrigo M, Hartel U, Kuhlenbeck H, Freund H.J(1999). Surf. Sci. 423 ,90.

[82] Nygren M.A., Petterson L G M(1996). J. Chem. Phys.105 ,9339.

[83]Giamello E, Paganini M C, Chiesa M , Murphy D M, Pacchioni G, Sovac R, Rockenbauer A(2000).J .Phys. Chem. B 104,1887.

[84] Paganini M, Chiesa M, Giamello E , Coluccia S, Martra G, Murphy D M , Pacchioni G(1999).Surf. Sci. 421,246

[85] Shalabi A S, El-Mahdy A M, Eid Kh M, Kamel M A(1999). Model. Simul. Mater. Eng. 7,1.

[86] Abbet S, Riedo E, Brune H, Heiz U, Ferrari A M, Giordano L, Pacchioni G (2001). J. Am.Chem. Soc. 123 ,6172.

[87] Ferrari A M, Pacchioni G(1996). Int. J. Quantum Chem. 58,241

Table 1:

Calculated parameters for the adsorption complexes of Cu, Ag and Au atoms on regular O^{2-} sites as well as the defect (F_S^0 and F_S^+) on terrace, edge, and oxygen corner of MgO and BaO (001) surfaces.

Oxide	Metal	Terrace						Edge						Corner					
		O^{2-}		F_S^0		F_S^+		O^{2-}		F_S^0		F_S^+		O^{2-}		F_S^0		F_S^+	
		d(M–S)	De (eV)	d(M–S)	De (eV)	d(M–S)	De (eV)	d(M–S)	De (eV)	d(M–S)	De (eV)	d(M–S)	De (eV)	d(M–S)	De (eV)	d(M–S)	De (eV)	d(M–S)	De (eV)
MgO	Cu	1.99	-0.541	1.62	-1.351	1.67	-2.677	2.01	-2.206	1.48	-1.564	1.60	-2.773	1.87	-1.836	1.35	-2.498	1.34	-2.507
	Ag	2.73	-0.394	1.84	-1.045	1.91	-2.393	2.40	-0.573	1.87	-1.260	1.81	-2.550	2.18	-1.211	1.59	-2.221	1.56	-2.292
	Au	2.48	-0.557	1.70	-2.220	1.71	-3.308	2.32	-2.811	1.76	-2.382	1.64	-3.513	2.16	-1.147	1.43	-3.142	1.40	-3.140
BaO	Cu	1.95	-1.619	1.46	-3.086	1.46	-3.225	1.89	-2.288	1.41	-2.834	1.39	-3.037	1.81	-3.065	0.90	-3.149	1.75	-2.285
	Ag	2.33	-1.048	1.88	-2.576	1.88	-2.713	2.22	-1.426	1.82	-2.420	1.80	-2.612	2.10	-2.329	1.48	-2.714	1.87	-1.978
	Au	2.28	-2.057	1.66	-4.087	1.65	-4.224	2.20	-2.461	1.60	-3.850	1.58	-4.036	2.10	-2.918	1.30	-4.069	2.06	-3.495

d(M–S): optimal distances in Å between adsorbed metals and surfaces site , De: optimal adsorption energies in eV.

Table 2:

Structural and energetic parameters of CO and MCO. d: optimal adsorption height. De: optimal adsorption energy. M: transition metal.

–De means the system is bound.

C-O	
d(C-O)Å	1.17
D(O)ev	-8.92

M-C-O	CU	Ag	Au
d(M-C) Å	1.93	4.20	2.07
d(C-O) Å	1.17	1.17	1.17
De(O)ev	-7.33	-7.66	-6.90
De(CO)ev	-0.39	-0.02	-0.40

Table 3:

Calculated parameters for the adsorption complexes of CO on the regular O^{2-} and defect (F_S^0 and F_S^+) sites of the oxide supports. d: optimal adsorption height. De: optimal adsorption energy.

-De means the system is bound. M: transition metal.

	FLAT			EDGE			CORNER		
Oxide	O^{2-}	F_S^0	F_S^+	O^{2-}	F_S^0	F_S^+	O^{2-}	F_S^0	F_S^+
MgO									
d(S-C)(Å)	4.11	0.56	0.94	1.51	0.57	0.94	1.40	0.31	0.55
d(C-O)(Å)	1.17	1.32	1.24	1.20	1.31	1.23	1.20	1.28	1.24
De(O)ev	-11.05	-6.87	-6.53	-6.14	-8.64	-9.53	-6.454	-8.548	-9.592
De(CO)ev	-0.46	0.32	-0.37	4.71	-0.06	-0.68	3.532	0.142	-0.412
BaO									
d(S-C)(Å)	4.23	-0.06	-0.04	1.398	0.345	0.273	1.32	0.25	0.216
d(C-O)(Å)	1.17	1.31	1.32	1.222	1.300	1.294	1.23	1.26	1.257
De(O)ev	-7.00	-6.85	-6.51	-5.42	-9.78	-9.57	-6.033	-10.303	-9.837
De(CO)ev	-0.16	-2.27	-2.51	3.15	-1.35	-2.06	1.249	-1.094	-1.698

Table 4:

Calculated parameters for the adsorption complexes MCO on the regular O^{2-} and defect (F_S^0 and F_S^+) sites of the oxide supports S. d: optimal adsorption height. De: optimal adsorption energy.

M: transition metal. -De means the system is bound.

	FLAT									EDGE									CORNER								
Oxide	O^{2-}			F_S^0			F_S^+			O^{2-}			F_S^0			F_S^+			O^{2-}			F_S^0			F_S^+		
	Cu	Ag	Au	Cu	Ag	Au	Cu	Ag	Au	Cu	Ag	Au	Cu	Ag	Au	Cu	Ag	Au	Cu	Ag	Au	Cu	Ag	Au	Cu	Ag	Au
MgO																											
d(S-M)(Å)	1.99	2.73	2.48	1.62	1.84	1.7	1.78	1.95	1.78	1.99	2.40	1.99	1.50	1.71	1.60	1.73	1.86	1.70	1.87	2.08	2.16	1.51	1.63	1.47	1.50	1.63	1.48
d(M-X)(Å)	1.83	2.32	2.09	1.89	2.17	2.09	1.99	2.31	2.23	1.87	2.21	1.87	1.90	2.17	2.10	2.00	2.34	2.30	1.86	2.05	1.95	1.99	2.35	2.31	2.00	2.35	2.28
d(X-O)(Å)	1.20	1.16	1.17	1.18	1.18	1.18	1.16	1.16	1.16	1.19	1.17	1.19	1.18	1.18	1.18	1.16	1.16	1.16	1.16	1.16	1.16	1.16	1.16	1.16	1.16	1.16	1.16
De(O)ev	-7.41	-7.46	-6.59	-8.00	-7.77	-7.76	-9.81	-10.05	-9.59	-7.49	-7.45	-6.82	-8.02	-8.35	-7.76	-9.82	-10.09	-9.67	-8.57	-9.13	-7.95	-8.48	-8.65	-8.42	-9.83	-10.04	-9.65
De(CO)ev	-0.83	-0.09	0.87	-1.20	-0.59	-0.54	-1.00	-0.66	-0.73	0.05	4.50	3.83	-1.14	-0.65	-0.66	-0.81	-0.54	-0.55	-1.74	-1.80	-1.66	-0.70	-0.43	-0.42	-0.75	-0.50	-0.51
De(MXO)ev	-1.05	-0.48	-0.37	-2.22	-1.7	-2.42	-3.29	-3.04	-3.63	-1.57	-0.63	-0.69	-2.32	-1.90	-2.64	-3.20	-3.08	-3.66	-3.19	-2.99	-2.40	-2.81	-2.64	-3.16	-2.88	-2.77	-3.24
BaO																											
d(S-M)(Å)	1.94	2.12	2.15	1.25	1.52	1.60	1.58	1.92	1.65	1.89	2.22	2.22	1.40	1.81	1.64	1.57	1.88	1.64	1.81	2.02	2.10	1.70	2.03	1.87	1.06	1.46	1.18
d(M-C)(Å)	1.75	2.02	1.99	1.97	2.20	2.45	2.13	2.77	2.80	1.86	2.04	1.95	1.97	2.97	3.02	2.14	3.15	3.09	1.84	2.04	1.95	4.15	2.98	3.84	3.18	3.32	3.44
d(C-O)(Å)	1.20	1.20	1.20	1.20	1.18	1.17	1.17	1.16	1.16	1.20	1.20	1.20	1.19	1.16	1.17	1.17	1.17	1.16	1.17	1.17	1.18	1.17	1.17	1.17	1.16	1.16	1.17
De(O)ev	-7.49	-7.34	-6.71	-7.23	-7.81	-7.61	-9.02	-9.78	-9.53	-7.53	-7.33	-6.80	-7.45	-7.89	-7.77	-8.83	-9.59	-9.31	-8.29	-8.26	-7.57	-7.58	-7.55	-8.25	-8.72	-9.55	-9.42
De(C O)ev	-1.09	-0.37	-0.50	-0.53	-0.01	-0.19	-0.26	-0.17	-0.17	-1.11	-0.42	-0.26	-0.33	-0.08	-0.07	-0.14	-0.10	-0.09	-1.68	-0.99	-1.22	0.51	0.39	0.52	-0.06	-0.06	-0.05
De(MCO)ev	-2.32	-1.34	-1.76	-3.23	-2.57	-3.88	-3.10	-2.86	-4.00	-3.01	-1.83	-2.31	-2.78	-2.48	-3.51	-2.79	-2.70	-3.72	-4.36	-3.30	-3.74	-2.25	-2.31	-3.14	-2.55	-2.48	-3.44

Table 5:

Total interaction energies of the S.M.CO system $E(i)P^{S\cdot\cdot M\cdot\cdot CO}P$, pairwise components $E(i)P^{S\cdot\cdot\cdot M}P$, $E(i)P^{S\cdot\cdot\cdot CO}P$, $E(i)P^{M\cdot\cdot CO}P$ and the non-additivity term E^{nadd} of CO adsorbed on Cu, Ag , Au deposited

on the defect-free (O^{2-} and defect-containing (F_S^0, F_S^+) surfaces of the alkaline earth oxide series. M: transition metal. All energies are given in eV.

	FLAT									EDGE									CORNER								
	O^{2-}			F_S^0			F_S^+			O^{2-}			F_S^0			F_S^+			O^{2-}			F_S^0			F_S^+		
Oxide	Cu	Ag	Au	Cu	Ag	Au	Cu	Ag	Au	Cu	Ag	Au	Cu	Ag	Au	Cu	Ag	Au	Cu	Ag	Au	Cu	Ag	Au	Cu	Ag	Au
MgO																											
E(i)S..M..CO	-1.44	-0.50	-0.77	-2.60	-1.71	-2.83	-3.67	-3.06	-4.04	-1.95	-0.64	-1.09	-2.71	-1.91	-3.04	-3.58	-3.09	-4.06	-3.57	-3.01	-2.81	-3.20	-2.65	-3.57	-3.26	-2.79	-3.65
E(i)S..M	-0.60	-0.41	-1.64	-1.41	-1.12	-2.29	-2.68	-2.39	-3.31	-2.00	-5.14	-4.93	-1.56	-1.26	-2.38	-2.77	-2.55	-3.51	-1.84	-1.21	-1.15	-2.50	-2.22	-3.14	-2.51	-2.29	-3.14
E(i)S..CO	-0.46	0.46	0.46	0.32	0.32	0.32	-0.37	-0.37	-0.37	4.71	4.71	4.71	-0.06	-0.06	-0.06	-0.68	-0.68	-0.68	3.53	3.53	3.53	0.14	0.14	0.14	-0.41	-0.41	-0.41
E(i)M..CO	-0.39	0.02	0.40	-0.39	-0.02	-0.40	-0.39	-0.02	-0.40	-0.39	-0.02	-0.40	-0.39	-0.02	-0.40	-0.39	-0.02	-0.40	-0.39	-0.02	-0.40	-0.39	-0.02	-0.40	-0.39	-0.02	-0.40
E^{nadd}	0.02	0.39	1.74	-1.13	-0.89	-0.46	-0.24	-0.28	0.04	-4.28	-0.20	-0.48	-0.70	-0.58	-0.19	0.26	0.16	0.54	-4.89	-5.32	-4.79	-0.46	-0.56	-0.16	0.04	-0.07	0.31
BaO																											
E(i)S..M..CO	-2.71	-1.36	-2.17	-3.62	-2.59	-4.28	-3.48	-2.88	-4.40	-3.40	-1.84	-2.72	-3.40	-2.50	-3.92	-3.18	-2.71	-4.12	-4.75	-3.32	-4.14	-2.08	-1.69	-2.85	-2.63	-2.03	-0.81
E(i)S..M	-1.61	-0.99	-1.67	-3.09	-2.58	-4.09	-3.22	-2.71	-4.22	-2.29	-1.43	-2.46	-2.83	-2.42	-3.85	-3.04	-2.61	-4.04	-3.06	-2.33	-2.92	-3.15	-2.71	-4.07	-2.88	-2.44	-3.79
E(i)S..CO	-0.16	0.16	0.16	-2.27	-2.27	-2.27	-2.51	-2.51	-2.51	3.15	3.15	3.15	-1.35	-1.35	-1.35	-2.06	-2.06	-2.06	1.25	1.25	1.25	-1.09	-1.09	-1.09	-1.70	-1.70	-1.70
E(i)M..CO	-0.39	0.02	0.40	-0.39	-0.02	-0.40	-0.39	-0.02	-0.40	-0.39	-0.02	-0.40	-0.39	-0.02	-0.40	-0.39	-0.02	-0.40	-0.39	-0.02	-0.40	-0.39	-0.02	-0.40	-0.39	-0.02	-0.40
E^{nadd}	-0.55	0.19	0.06	2.12	2.27	2.48	2.63	2.36	2.73	-3.87	-3.55	-3.00	1.16	1.28	1.69	2.31	1.98	2.38	-2.54	-2.22	-2.07	2.55	2.14	2.72	2.33	2.12	5.08

Table 6:

	FLAT			EDGE			CORNER		
O	O^{2-}	F_S^0	F_S^+	O^{2-}	F_S^0	F_S^+	O^{2-}	F_S^0	F_S^+
M	10.590	7.192	6.162	8.078	5.807	7.978	7.209	5.914	6.404
B	6.840	4.588	3.999	5.7947	5.658	4.731	4.505	6.432	5.362

The calculated released energy ΔE for adsorption reactions of CO on O^{2-}, F_S^0, and F_S^+ sites of the oxide support. $+\Delta E$ implies that the reaction is endothermic.   All energies are given in eV

Table 7a:

Highest occupied molecular orbital's (HOMOs) and lowest unoccupied molecular orbital's (LUMOs) of MCO fragments. All energies are given in eV.

	CuCO	AgCO	AuCO
HOMO	-5.259	-5.063	-4.392
LUMO	-2.761	-1.627	-2.859

Table 7b:

 Tops of the valance bands (V.B.), and the bottoms of conductions bands (C.B.), of defect-free surfaces of MgO and BaO crystals.

 As well as the highest occupied molecular orbitals (HOMOs) and the lowest unoccupied molecular orbitals (LUMOs) of the defect-containing

 surfaces before and after the adsorption of TM/MO systems. All energies are given in eV.

Oxide	Metal	O^{2-}		F_S^0		F_S^+	
		V.B.	C.B.	HOMO	LUMO	HOMO	LUMO
MgO	CO/MgO	-7.068	-3.779	-5.362	-3.812	-10.747	- 8.403
	Cu	-4.616	-4.211	-4.781	-3.863	-10.654	-7.273
	Ag	-4.929	-3.725	-4.591	-3.808	-10.534	-6.868
	Au	-5.000	-3.785	-4.683	-3.864	-10.613	-7.069
BaO	CO/BaO	-4.024	-3.135	-3.806	-3.079	-7.166	-6.472
	Cu	-3.767	-3.188	-3.742	-3.118	-6.880	-5.702
	Ag	-3.743	-3.193	-3.697	-3.110	-6.777	-5.149
	Au	-3.755	-3.188	-3.650	-3.149	-6.786	-5.157

Table 7c:

 Tops of the valance bands (V.B.), and the bottoms of conductions bands (C.B.), of defect- free surfaces of MgO and BaO crystals.

 As well as the highest occupied molecular orbitals (HOMOs) and the lowest unoccupied molecular orbitals (LUMOs) of the defect-containing

surfaces before and after the adsorption of CO molecule. All energies are given in eV.

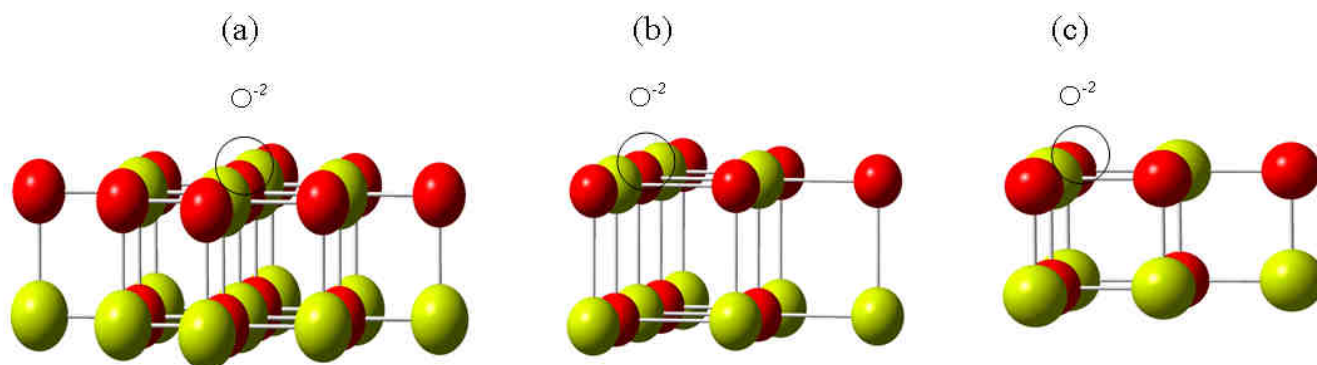| Oxide	Metal	O^{2-}		F_S^0		F_S^+	
		V.B.	C.B.	HOMO	LUMO	HOMO	LUMO
MgO	Free	-7.061	-3.724	-5.738	-3.795	-10.518	- 6.734
	Cu	-5.817	-3.882	-4.635	-3.929	-10.766	-7.112
	Ag	-5.451	-3.617	-4.597	-3.915	-10.714	-7.119
	Au	-6.242	-3.867	-4.828	-3.890	-10.752	-7.385
BaO	Free	-4.000	-3.118	-3.719	-3.173	-6.980	-5.115
	Cu	-4.052	-3.181	-3.610	-3.186	-6.824	-5.147
	Ag	-4.121	-3.186	-3.610	-3.180	-6.837	-5.150
	Au	-4.140	-3.181	-3.613	-3.207	-6.837	-5.147

Fig. 1.Schematic representation of low coordinated sites with different coordination at the surfaces of MgO (001)and BaO (001). (a)terrace; (b) edge; (c) corner. Red spheres: O^{-2}; Yellow spheres: Mg^{+2}, Ba^{+2}
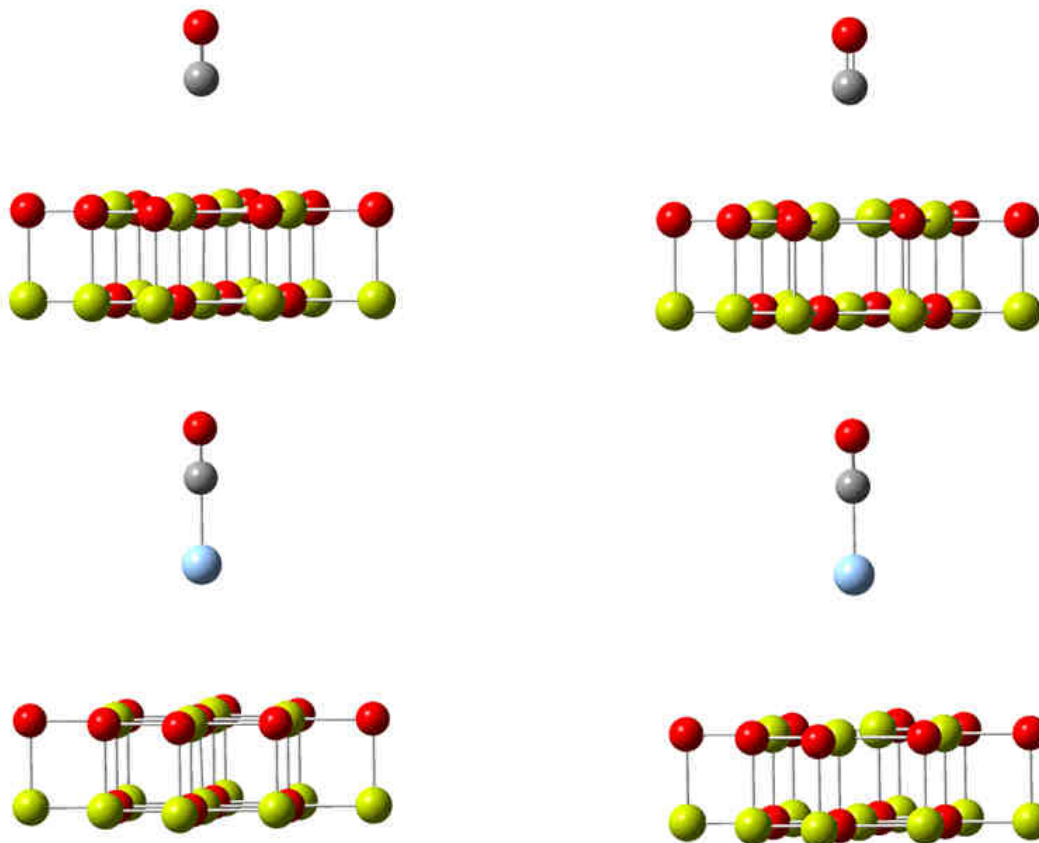

Fig. 2. A representative sketch of CO adsorbed on metal oxide (up row) and on deposited metal atoms (bottom row) of the defect-free (left) and defect-containing (right) surfaces of oxide supports.
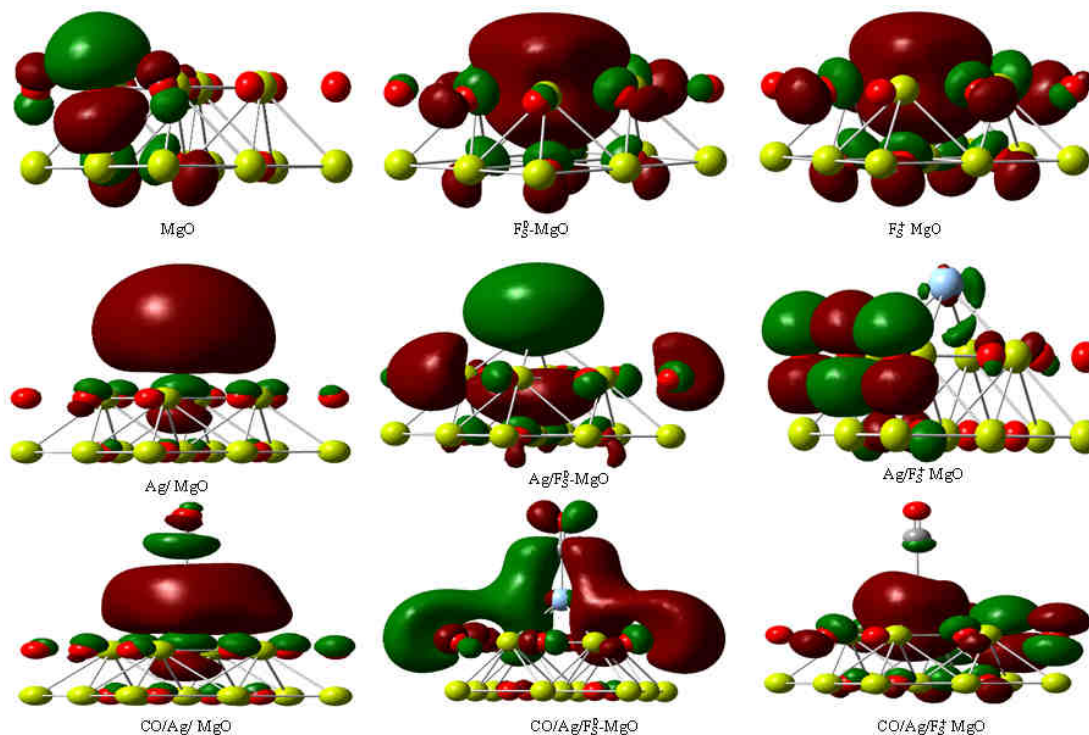
Fig. 3. (a) Plots of the HOMOs of the various sites of clean MgO (upper row), Ag/MgO (second row, Ag as a representative), CO/Ag/MgO (the last row). (b) Like (a) but for BaO, Red spheres: O^{2-}; yellow spheres: MgO^{2+}; cyan sphere: Ag; gray sphere: C atom.
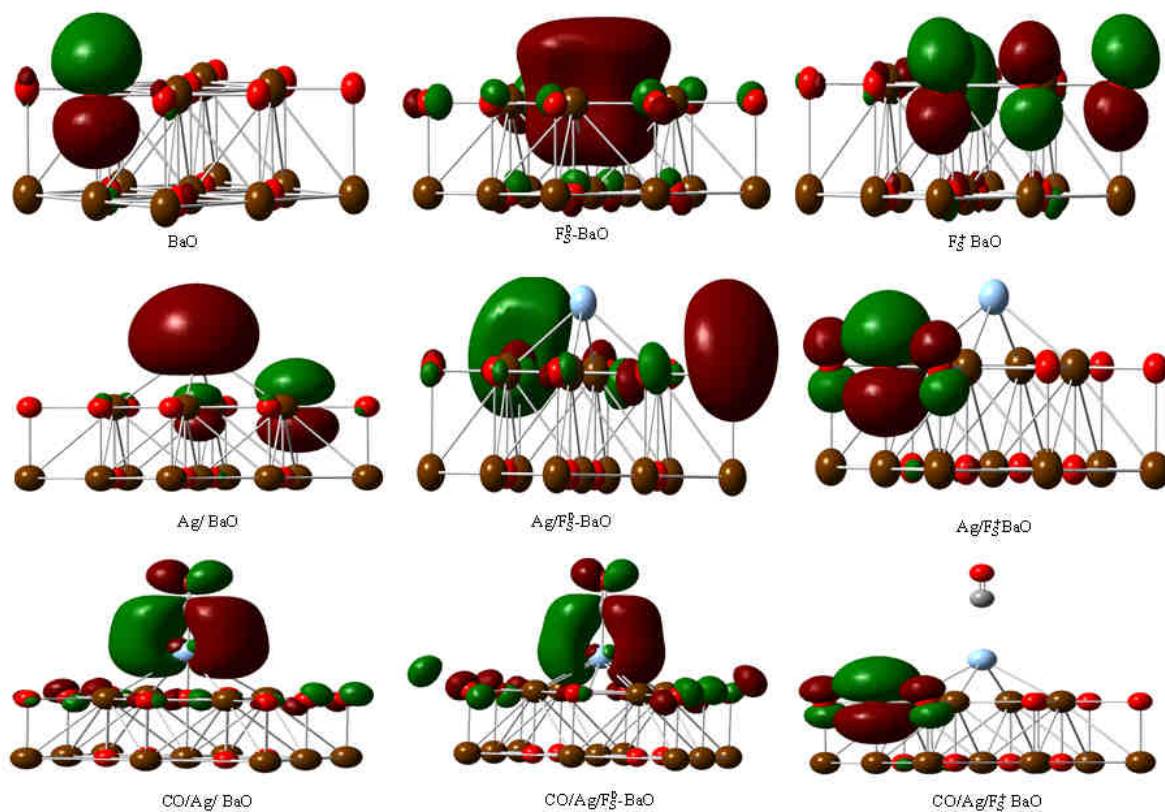
Fig. 3. (Continued)
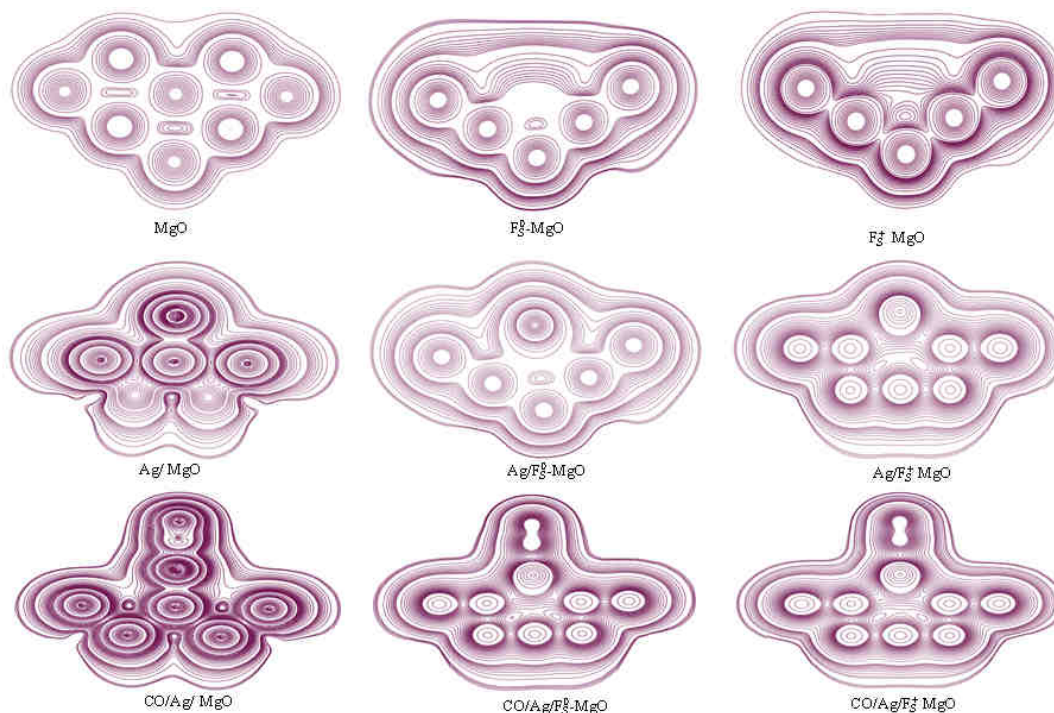
Fig. 4. (a) Total charge-density contours in the (0 0 1) plane of MgO clean surface (upper row), Ag/MgO (row 2), CO/Ag/MgO (row 3) of defect-free (right column) and defect-containing surfaces (F_S^0: middle column, and F_S^+: left column). (b) Like (a) but for BaO.
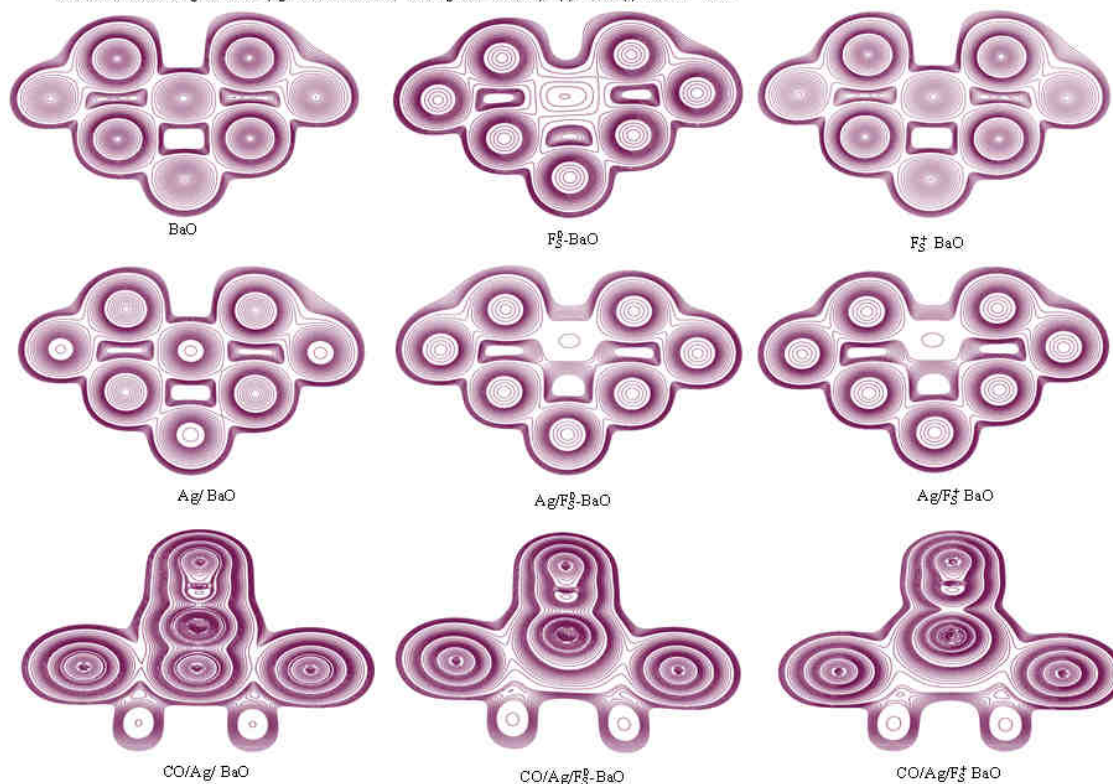
Fig. 4. (Continued)
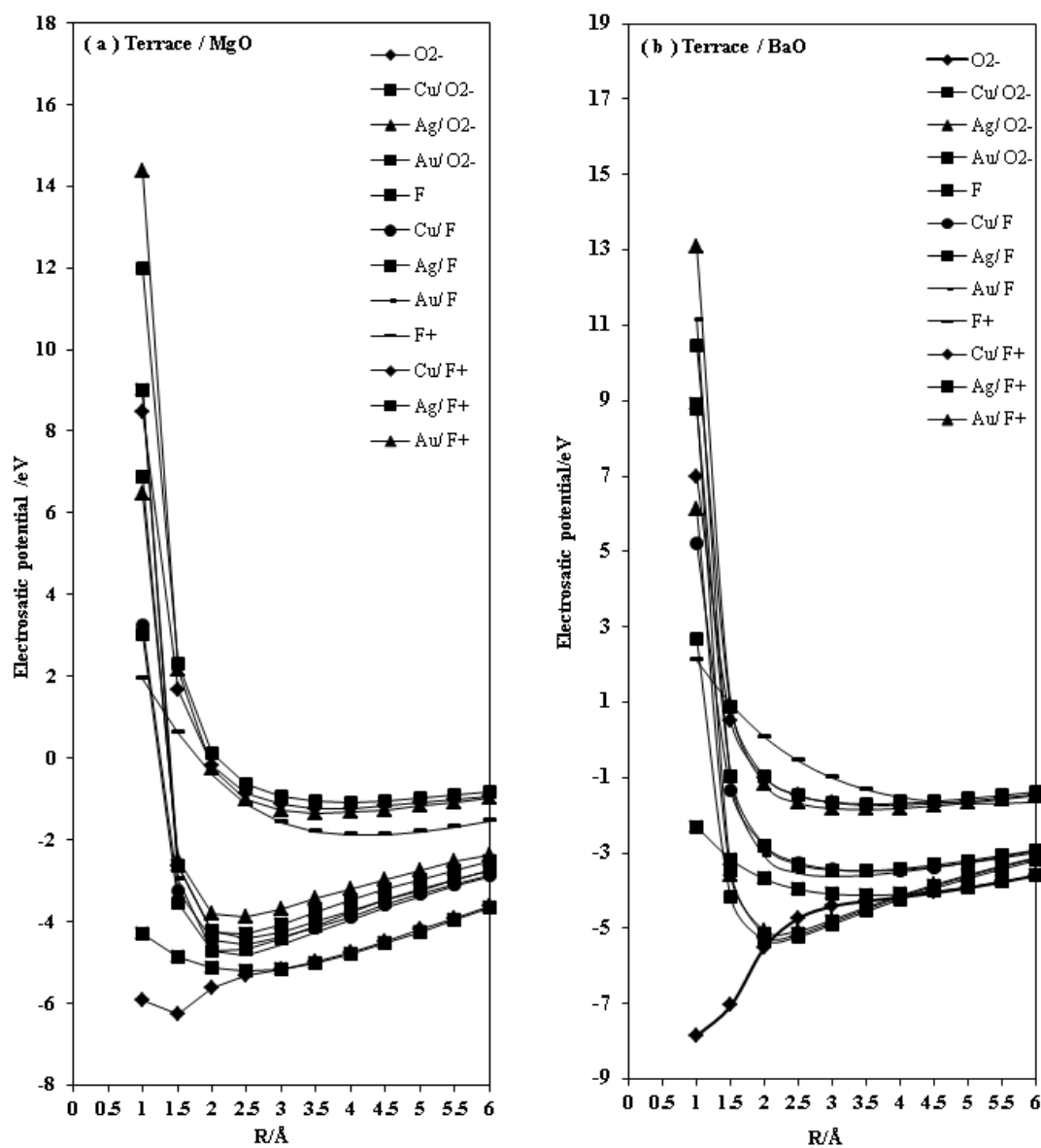
Fig. 5 a: Electrostatic potential curves over the defect-free (O^{2-}) and defect containing surfaces F_s^0 and F_s^+ centers at the terrace sites of the MgO and BaO surface.
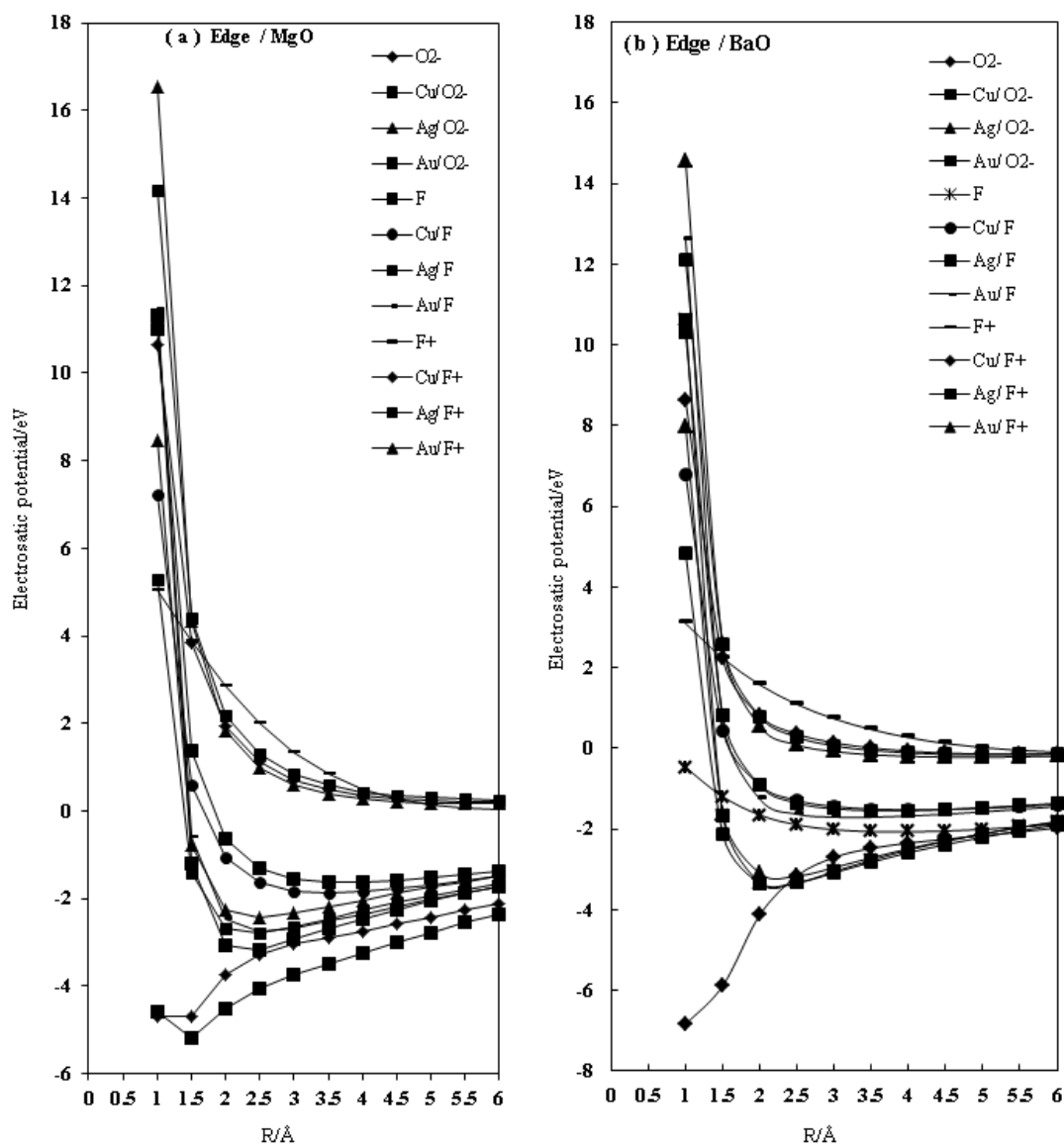
Fig. 5b : Electrostatic potential curves over the defect-free (O^{2-}) and defect containing surfaces F_s^0 and F_s^+ centers at the edge sites of the MgO and BaO surface.
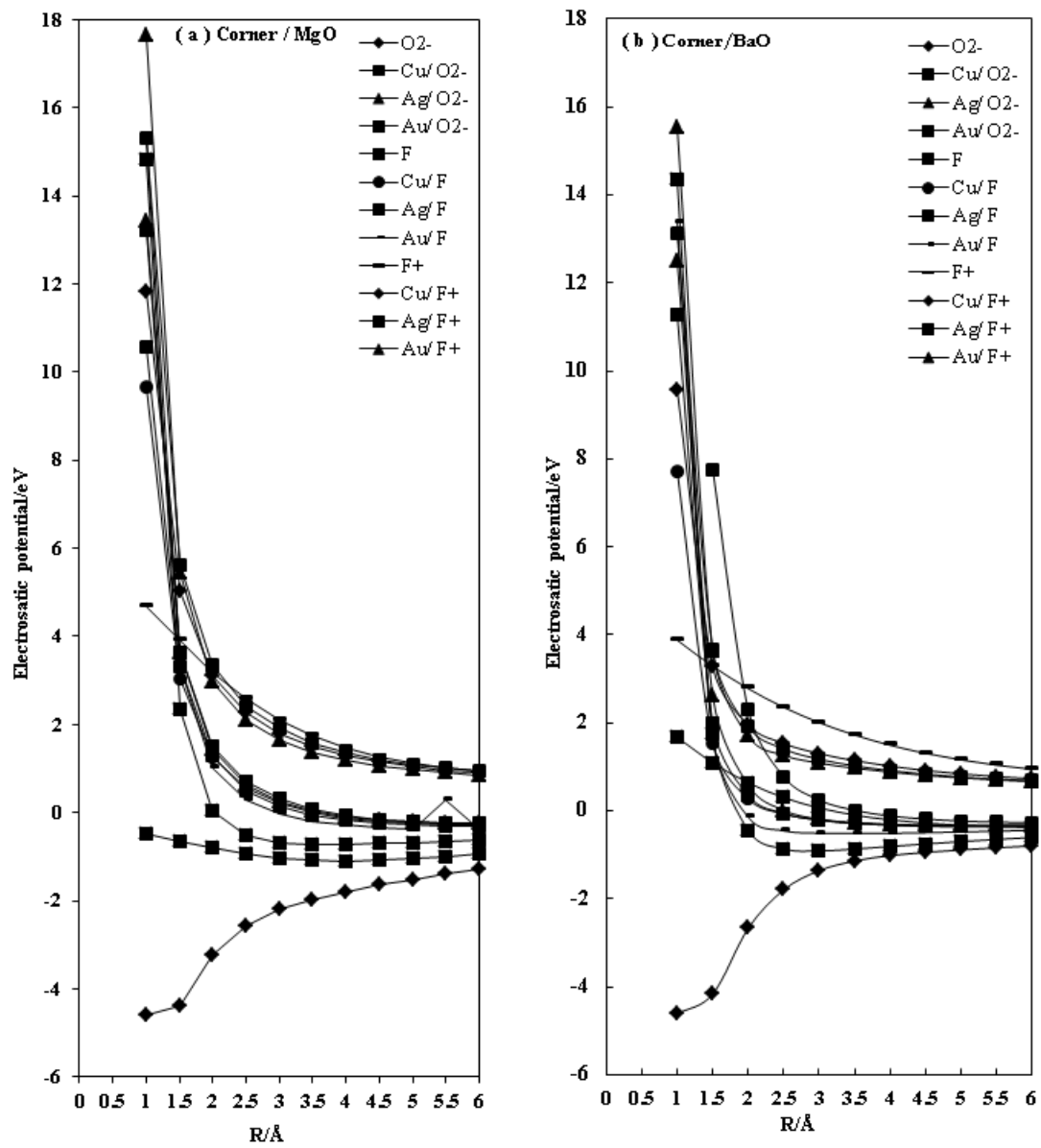
Fig. 5c : Electrostatic potential curves over the defect-free (O^{2-}) and defect containing surfaces F_S and F_S^+ centers at the corner sites of the MgO and BaO surface.
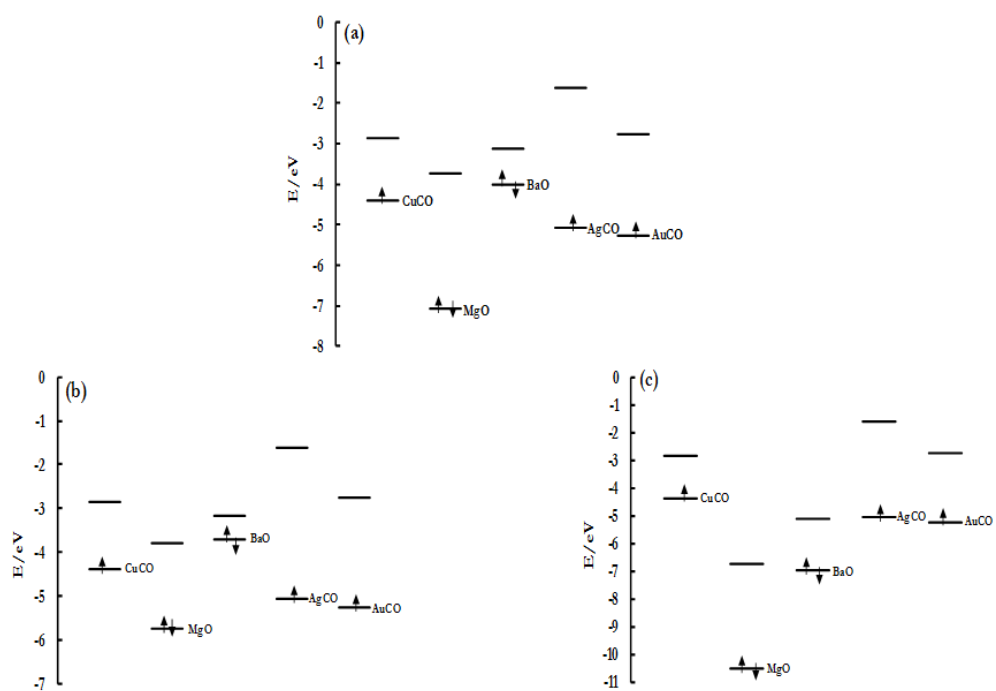
Fig. 6.(a) Molecular orbital energy levels (HOMOs and LUMOs) of MCO fragments deposited on O^{2-} sites of oxide supports. (b) Molecular orbital energy levels (HOMOs and LUMOs) of MCO fragments deposited on F_S sites of oxide supports. (c) Molecular orbital energy levels (HOMOs and LUMOs) of MCO fragments deposited on F_S^+ sites of oxide supports.

The IISTE is a pioneer in the Open-Access hosting service and academic event management. The aim of the firm is Accelerating Global Knowledge Sharing.

More information about the firm can be found on the homepage:
http://www.iiste.org

CALL FOR JOURNAL PAPERS

There are more than 30 peer-reviewed academic journals hosted under the hosting platform.

Prospective authors of journals can find the submission instruction on the following page: http://www.iiste.org/journals/ All the journals articles are available online to the readers all over the world without financial, legal, or technical barriers other than those inseparable from gaining access to the internet itself. Paper version of the journals is also available upon request of readers and authors.

MORE RESOURCES

Book publication information: http://www.iiste.org/book/

IISTE Knowledge Sharing Partners

EBSCO, Index Copernicus, Ulrich's Periodicals Directory, JournalTOCS, PKP Open Archives Harvester, Bielefeld Academic Search Engine, Elektronische Zeitschriftenbibliothek EZB, Open J-Gate, OCLC WorldCat, Universe Digtial Library , NewJour, Google Scholar